IJCRT.ORG ISSN : 2320-2882

INTERNATIONAL JOURNAL OF CREATIVE RESEARCH THOUGHTS (IJCRT)

An International Open Access, Peer-reviewed, Refereed Journal

Impact of number of deposition cycle number on the structural, surface morphology and some electrical, optical properties of FeSe thin film prepared by SILAR method

Kailas C. Shinde[1], Yogesh S. Sakhare[*2] and Raghavendra J. Topare[1]

[1]Department of Physics, Yogeshwari Mahavidyalaya, Ambajogai, Dist: Beed.

[2]Department of Physics, Late Pundalikrao Gawali Arts and Science College, Shirpur (Jain), Dist: Washim.

Abstract

Optoelectronic tricks are made by the semiconductor composite and their mixtures due to their direct and indirect optical band gap energy. Here, FeSe thin films were manufactured by SILAR technique on well cleaned glass substrates at room temperature. The Prepared thin film was characterized by X-ray analysis and Uv-Visible spectroscopy. The X-ray diffraction studies revealed that, FeSe thin film is nanocrystalline in nature with hexagonal structure. The optical studies of FeSe thin film shows that the maximum absorption observed in the visible region and it can be used as an absorber in the visible region for optoelectronic devices. The direct or indirect band gap energy are varying from 2.95 eV to 2.63 eV with number of deposition cycle from 50 to 250 and thickness varies from 79 to 276 nm. The room temperature electrical resistivity were of the order of from 42 x 10^4 (Ω-cm) to 16 x 10^4 (Ω-cm).

Key words: - SILAR, thin film, Magnesium selenide and electrical resistivity

1.Introduction

The successive ionic layer adsorption and reaction (SILAR) technique was primary introduced in 1985 by Nicolau for the deposition of ZnS and CdS [1] and Ristov et al. for the deposition of Cu_2O thin films [2]. In this method, the sample is dipped one by one into two given solution and wash down in between with distilled water to get rid of the loosely bound species. In this process, one SILAR round contains of adsorption of the cation precursor, rinsing with water, adsorption of anion precursor, followed by reaction and another rinsing. The progress rates of the thin films in the SILAR method have varied between a quarter and a half of a

monolayer, depending on the experimental situation [3]. Thin films have attracted much interest because they possess unique properties [4]. Several physical methods and chemical deposition techniques were used for the growth of thin films on substrates. These deposition methods include electrodeposition [5], chemical bath deposition [6], magnetron sputtering, chemical vapor deposition, spray pyrolysis, thermal evaporation [7], molecular beam epitaxy, ion beam deposition, electron beam evaporation, atomic layer epitaxy, the spin coating method [8], the pulsed laser deposition method, and the successive ionic layer adsorption and reaction (SILAR) technique. Thin films could be used in lasers, cathodic ray tubes, solar cells [9], infrared windows, ultraviolet light-emitting diodes, sensors [10], supercapacitors, and biological and optoelectronic applications [11].Iron selenide (FeSe) has gained significant attention as a semiconducting thin film material due to its intriguing electronic properties, including tuneable bandgap, excellent charge carrier mobility, and compatibility with various substrates [12-14]. FeSe primarily demonstrates two crystalline structures a tetragonal phase and a hexagonal phase [15]. Researcher investigated how deposition potential influences the properties of electrochemically grown iron selenide thin films, revealing hexagonal wurtzite structure with well-defined morphology [16]. Thin films of FeSe and $FeSe_2$ found to be p-type semiconductor with an energy gap value in the range between 1.23 and 1.08 eV which make them interesting for its applications in superconductors, photovoltaic and optoelectronics devices [17-18]. Among all these deposition method successive ionic layer adsorption and reaction (SILAR) is low cost deposition method. For this particular study we have preferred SILAR method for the deposition of FeSe thin film. Because SILAR method is a simple, low cost, convenient and useful for large area industrial application. SILAR does not require high quality substrates nor does it require vacuum at any stage, which is a great advantage if the sample will be used for industrial application, the deposition rate and the thickness of the film can be easily controlled over a wide range by changing the deposition cycles [19]. To the best of our knowledge, it is the first report on the effect of immersion cycles on the properties of FeSe thin films by SILAR. The present paper deals with the preparation of FeSe thin films and characterization of the films by XRD, FE-SEM and study of their optical and electrical properties.

2. Synthesis

Scheme of SILAR method

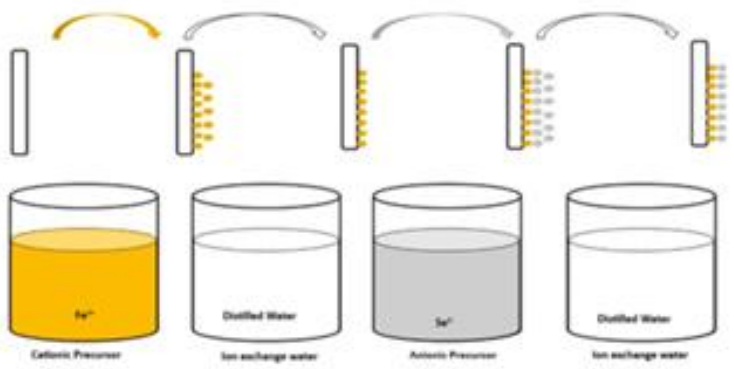

Figure 1: the scheme of SILAR techniques for the deposition of FeSe thin films.

SILAR method, to develop thin film the substrate is immersed repeatedly into separately placed cationic and anionic precursor alternately. To eliminate freely bound variety, after each precursor immersion, the substrate is rinsed in de-ionized water as shown in figure 1. For the current work the glass slides of size 75×25×1 mm was used as substrates. Before actual deposition cleaning of the substrate is very important as it affects the development system. Initially, the slides were washed with liquid detergent, then boiled in concentrated acid for 2 hour and then kept in it for next 48 hours. The substrates were then washed with double distilled water and cleaned in ultrasonic cleaner for 10 min. Finally, the substrates were dried using AR grade acetone. The 0.13 M, Na_2SeSO_3 solution was prepared by mixing 10 g selenium metal powder with 100 g anhydrous sodium sulphite in 500 ml of distilled water with constant stirring for 10 h at 80^0C. It was then sealed and kept overnight, since on cooling, a little selenium separated out from the solution. Finally, it was filtered to get 0.13 M clear solution of Na_2SeSO_3. The deposition of FeSe films was done at room temperature in a reactive solution prepared in a beaker. Glass substrates were immersed in the 80 ml of $Fe(NO_3)_3.9H_2O$ solution of Molar concentration 0.6 M for 20s, after each precursor immersion the substrate is rinsed in de-ionized water. It was then to immersed in 80 ml of freshly prepared Na_2SeSO_3 solution for 20 s and again then substrate is rinsed in de-ionized water for removal of freely bound particle. This forms one complete SILAR deposition cycle. Deposition cycles were varied from 50 to 250 cycles in the step of 25 cycles and as thickness increases from 79 nm to 276 nm respectively.

The structural studies were carried out using Rigaku MiniFlex II diffractometer, with Cu-Kα radiation of wavelength 1.5405 A°. The morphological study of the film was carried out using scanning electron microscopy (SEM) with a Park Scientific Instruments and SEM/EDAX with JOEL's JSM -7600F. The dc two-point probe method of dark electrical resistivity was used to study the variation of resistivity with temperature. The optical characteristics were studied using Lambda 25 UV-VIS spectrophotometer (PerkinElmer) to find band gap energy of FeSe thin films. In the present work, thickness of the film was measured by gravimetric weight difference method using the relation,

$$t=m/(\rho \times A) \quad (1)$$

where m is the mass of the film deposited on the substrate in gram, A is the area of the deposited film in cm^2 and ρ is the density of the deposited material in bulk form. The thickness of FeSe thin film with varying number of deposition cycle is shown in table 1.

Sr.No.	No. of SILAR Cycles	Thickness (nm)	Growth rate nm/cycle
1	50	59	1.58
2	100	112	1.12
3	150	167	1.11
4	200	204	1.02
5	250	276	1.10

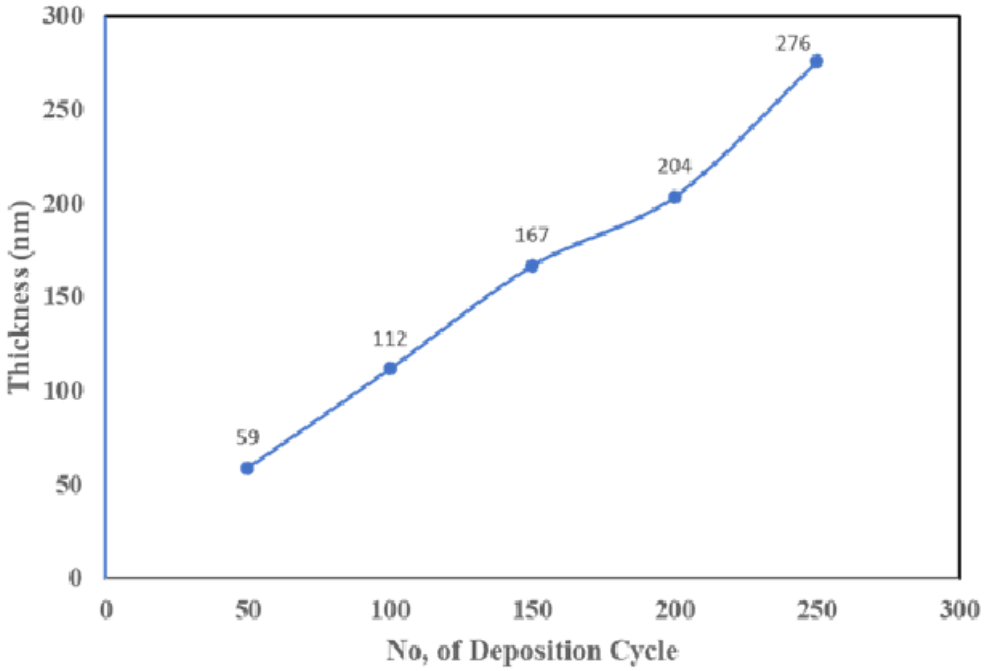

Fig:2 Variation of FeSe thin films thickness (nm) with number of deposition cycle (immersing cycle)

3. Result and Discussion:

3.1 XRD

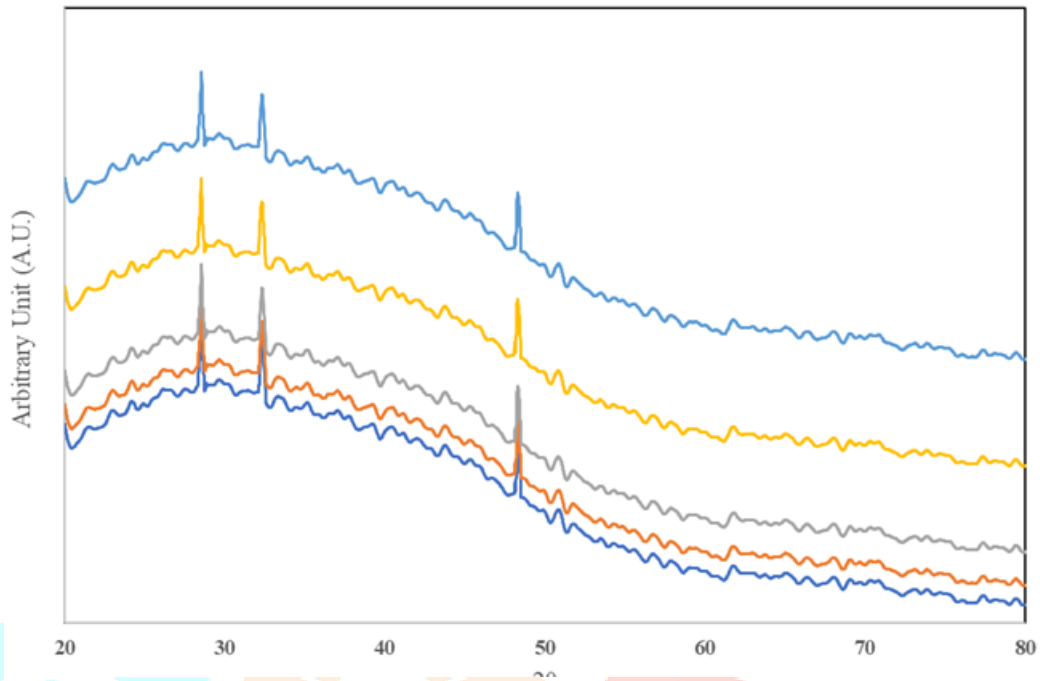

Figure 3: x-ray diffraction patterns of FeSe thin films of thickness varying from 54 nm to 296 nm.

In order to study the growth rate, SILAR deposited FeSe thin films were deposited for various from 50 to 250 immersion cycles on glass substrate. Figure 3 represent FeSe film thickness as a function of the immersion cycles (number of deposition cycle) and it varies from 79 nm to 276 nm. It is found that the film thickness increases with the deposition cycles. In order to study crystal structure of FeSe thin film deposited by SILAR method, X-ray diffraction of the film on the glass substrate was studied. The XRD patterns clearly showed the influence of the immersion cycles on the crystallinity of the films. For all FeSe films, the hexagonal crystal structure characterized with (101) planes as preferred orientation, is identified. The peaks at 2θ =28.61,32.33 and 48.22 referred to the (101), (002) and (200) orientation of the hexagonal phase of the FeSe thin films. The XRD peaks corresponding to 28.61 FeSe becomes more intense as number of immersion cycles increases from 50 to 250. No shift in the peak position was found with the increase of immersion cycles. The crystalline size (D) of the films has been evaluated the high intensity peals 2θ= 28.61 by using Scherrer's formula,

$$D = \frac{k\lambda}{\beta cos\theta}$$

Where k is constant is the wavelength of X-ray, β is the full width at half of the peak maximum in radians and θ is Bragg's angle. It is observed that the crystallite size increases from 59 nm to 94 nm as immersion cycles increase from 50 to 250.

3.2 SEM/EDEX

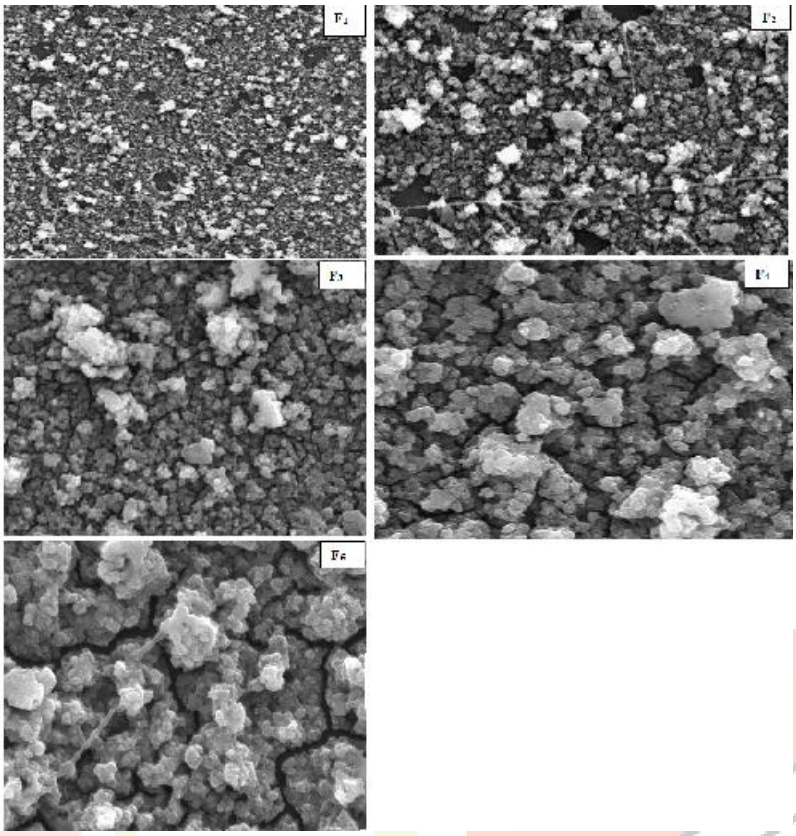

Figure 4: Scanning electron micrograph image of FeSe thin films of thickness 54 nm to 296 nm.

Field emission scanning electron microscopy (FESEM) was used to investigate the effect of the immersion cycle on thin film surface properties because the surface properties directly affect the electrical and optical properties of the films. The FESEM image of the FeSe thin film deposited with different immersion cycles are present in figure 4. it is observed from figure 3a that all the thin films were homogenous, without cracks or holes and with dense surface morphology covering entire substrate surface area. It can also be seen from FESEM image that the films were composed of a large number of spherical nanoparticles. Improvement in the crystallinity was found with increase of immersion cycles.

3.3 Optical Properties

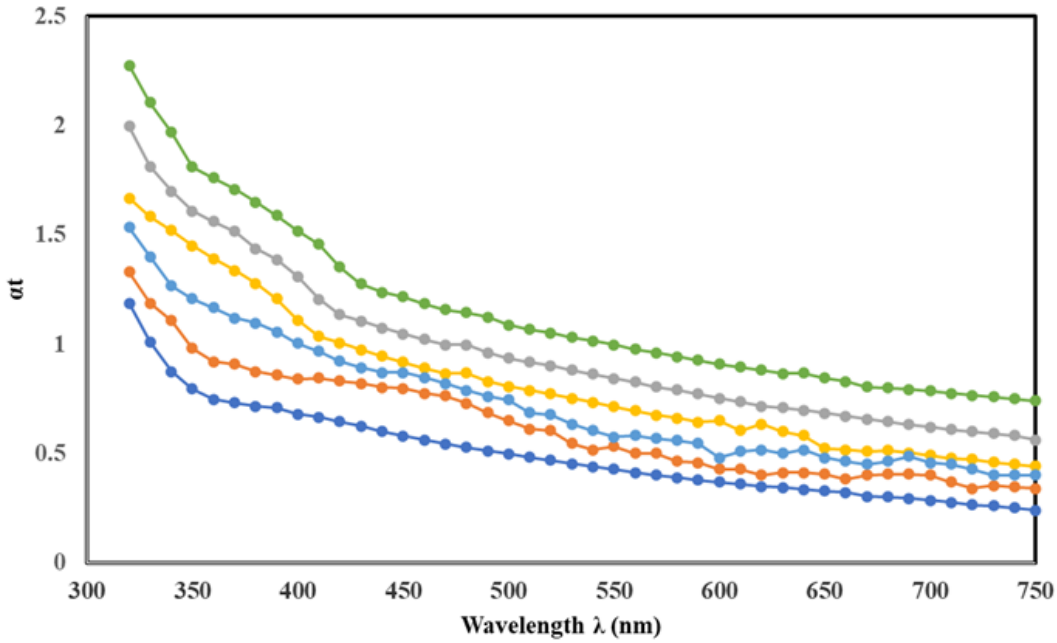

Figure 5: Polts of Optical absorption (αt) versus wavelength λ (nm) of FeSe thin films of thickness 54 nm to 296 nm.

Uv-visible spectra are produced by electronic transitions of the molecules that absorb energy in the form of ultraviolet or visible light going from the ground electronic state into excited states, from where the energy is further dissipated by non-radioactive processes such as collisions with other molecules. The optical absorption measurement of the iron selenide thin film deposited by SILAR technique onto glass substate was carried out in the wavelength range 350 to 850 nm at room temperature. The maximum absorption in the visible region is observed shows that the iron selenide thin film can be used as absorber in the visible region for the optoelectronic devices. The optical band gap energy of iron selenide thin film was calculated by using the equation transition.

$$\alpha h\vartheta = A(h\vartheta - E_g)^n$$

Where α is a absorption coefficient, E_g is the energy band gap, a is a constant and n is equal to ½ for direct and 2 for indirect. The direct or indirect optical energy band gap E_g of FeSe thin film are found to be varying from 2.95 eV to 2.63 eV.

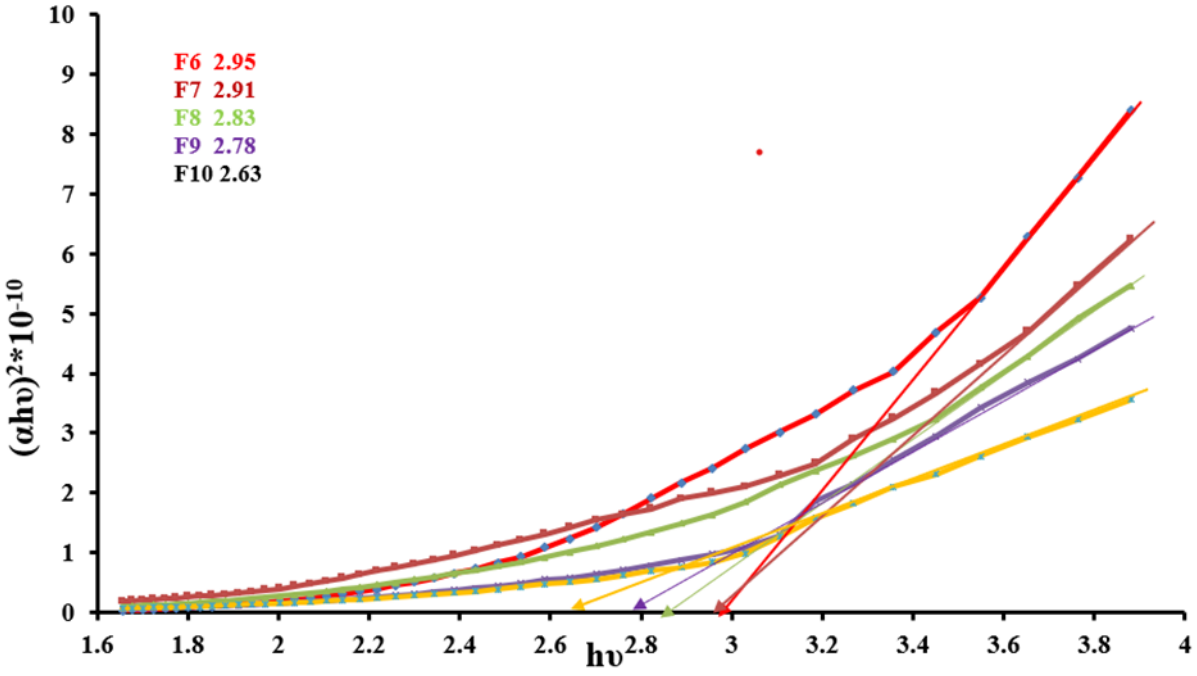

Figure 6: Plots of (αhν)2 versus hυ for FeSe films of thickness 54 nm to 296 nm.

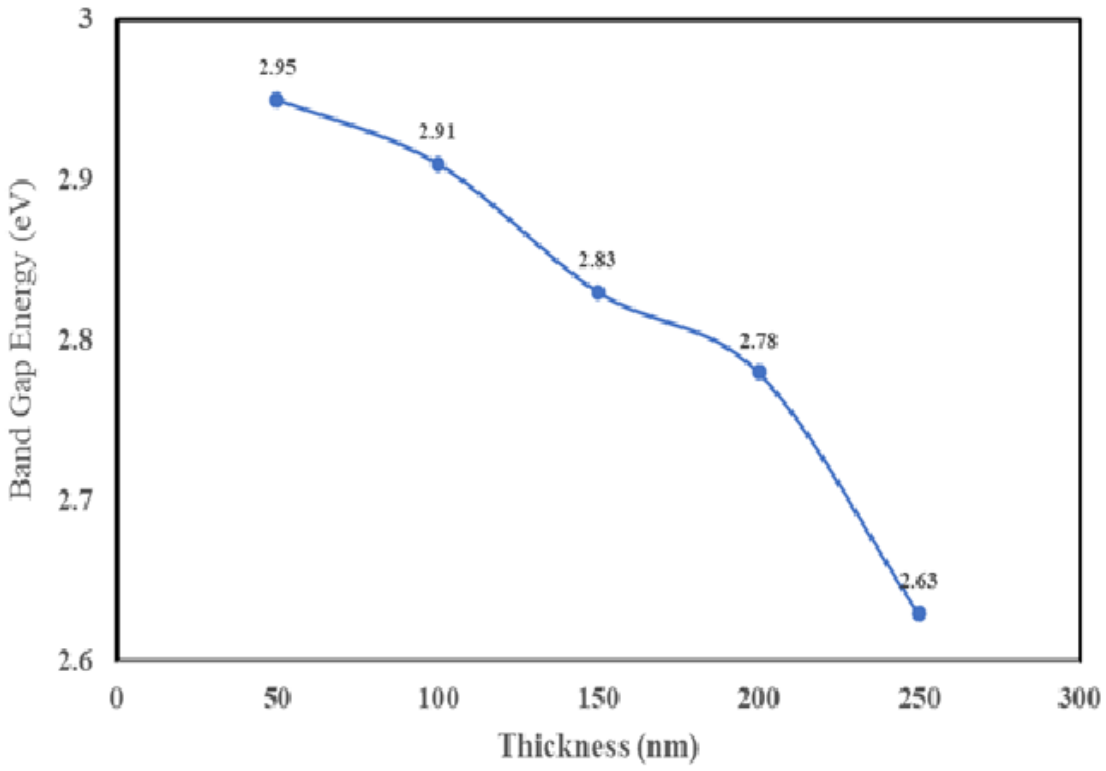

Fig:7 Variation of Optical Band Gap Energy (eV) of FeSe thin film with thickness (nm).

3.4 Electrical Properties

The electrical resistivity measurements showed that SILAR grown FeSe films are semiconducting in nature. It is also observed that the resistivity of FeSe decreases with increase in film thickness which may be due to improvement in crystallinity of the films. The thermal activation energy Ea was calculated by using relation

$$\rho = \rho_0 \frac{Ea}{KT}$$

Where, ρo is a parameter depending on the sample characteristics (thickness, structure etc.), Ea denotes the thermal activation energy of electrical conduction, K is Boltzmann's constant and T is absolute temperature. The activation energy is decrease with film thickness increases in both low and high temperature region.

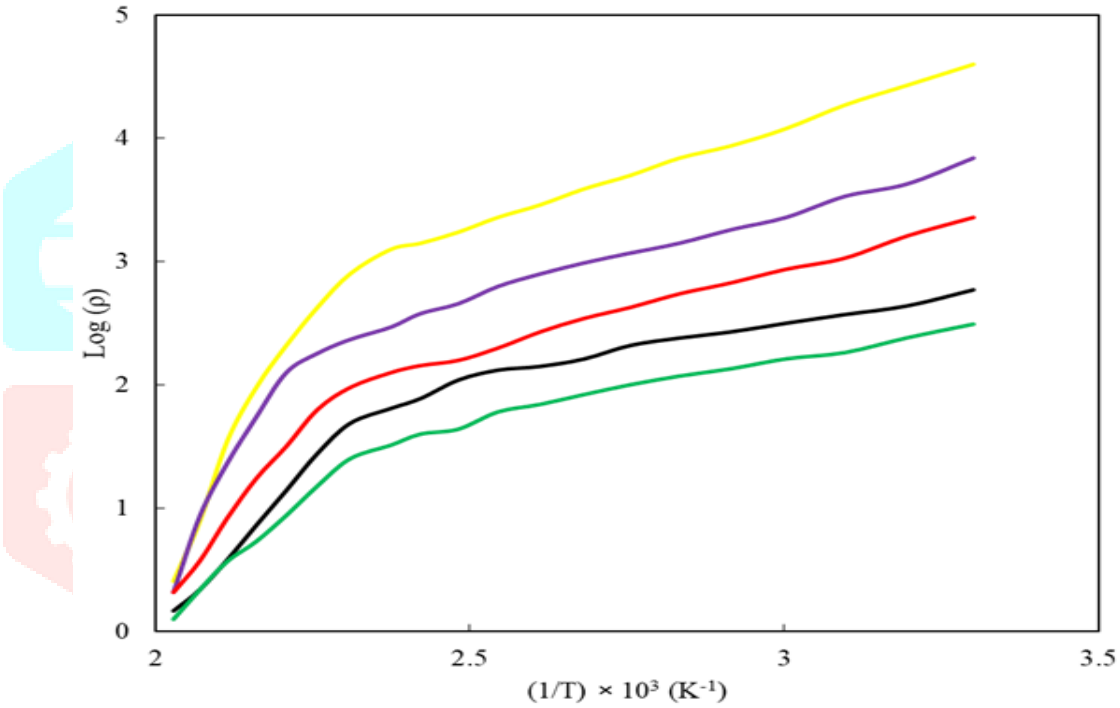

Figure 8: Variation of log (ρ) versus 1/T x 103 (K-1) for FeSe thin film at various number of deposition cycles.

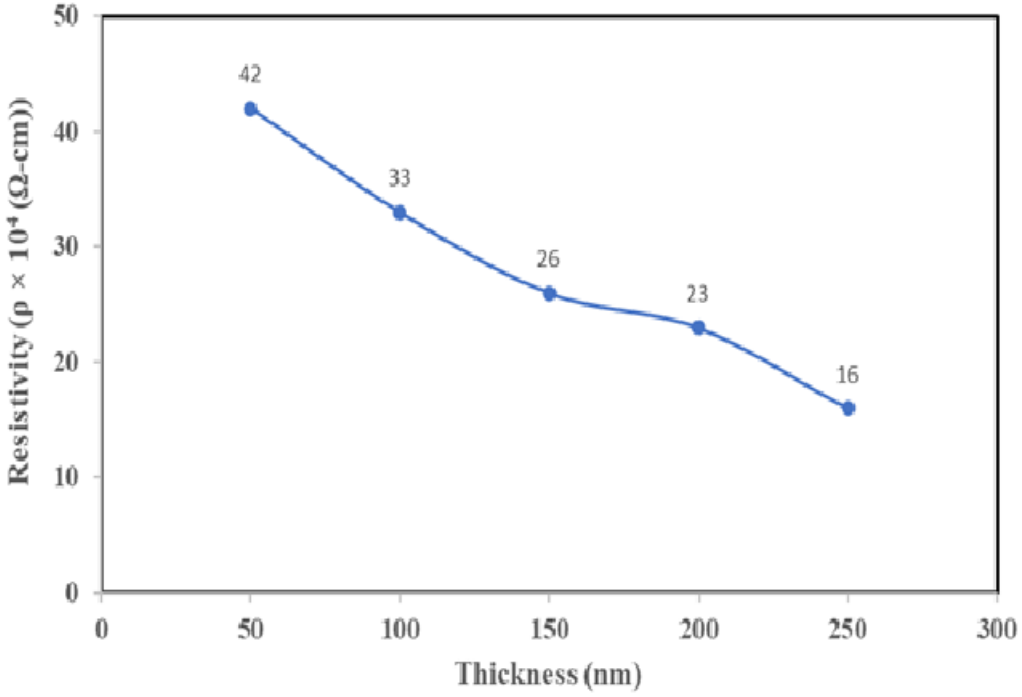

Fig:9 Variation of Resistivity (Ω-cm) of FeSe thin film at 373K temperature with film thickness (nm).

4.Conclusion

Good quality Iron selenide (FeSe) thin films were deposited onto glass substrate by using SILAR method as a function of immersion cycles varying from 50 to 250 in the interval of 50. Xrd analysis revealed the hexagonal structure of FeSe thin film. Peak intensity increases with immersion cycles and thus the crystalline quality of the films gets better and the crystallite size increases with increases of immersion cycles. Surface properties of deposited thin film were improved with increasing immersion cycles. The band gap energy values reduced from 2.95 to 2.63 eV with increases in the immersion cycles. Electrical studies showed that the films are semiconducting which may be used in optical and electrical devices.

Reference

[1] Y. Nicolau, Applied Surface Science. 1985; 22:1061

[2] Ristov M, Sinadinovski G, Grozdanov I. Thin Solid Films. 1985; 123:63

[3] B.R. Sankapal, R.S. Mane, C.D. Lokhande, Materials Research Bulletin.Vol. 35(12), 2000, 2027-2035

[4]. Harif, N.; Halina, M.; Hasrul, R.; Kazi, S.; Camellia, D.; Sopian, K.; Amin, N. Crystals 2021, 11, 73.

[5]. Megan, J.; Kreiml, P.; Mitterer, C. Materials 2022, 15, 926.

[6]. Ho, S.M.; Mandati, S.; Chandran, R.; Mallik, A.; Arif, S.; Deepa, K. Orient. J. Chem. 2019, 35, 1–13.

[7]. Bin,W.; Huang,W.; Lin,W.; Lee, H. Crystals 2021, 11, 1380.

[8]. Zaman, M.; Taru, C.; Dehury, K.; Rajaram, P. AIP Conf. Proc. 2018, 1953, 100066.

[9]. Ho, S.M. Makara J. Sci. 2017, 21, 119–124.

[10]. Mikayal, A.; Zarine, S.; Gohar, S.; Ladimir, A.; Artak, S. Chemosensors 2022, 10, 245.

[11] Istrate, A.; Vulpe, S.; Florin, N.; Lucia, M.; Cosmin, R.; Oana, T. Coatings 2021, 11, 1023.

[12] A.U.Ubale , Y.S.Sakhare, M.V.Bhute, M.R.Belkhedkar , A.Singh , Solid State Sci., 2013, 16:134

[13]. Qasrawi A.F., Toubasi A.J. Optik, 2023, 287:171173

[14]. NM S.S.B., Chandra Mohan R., Saravana Kumar S., Ayeshamariam A., Jayachandran M. Fluid Mech Open Acc, 2017, 4:6

[15]. Piperno L., Celentano G., Sotgiu G. Coatings, 2023, 13:1905

[16]. Thanikaikarasan S., Perumal R., Marjorie S.R. J. Alloys Compd., 2020, 848:156348

[17] X. Wu, Z.Zhang, J.Zhang, B.Li, Z.Ju, Y.Lu, B.Li, D.Shen, J. Appl. Phys.103 (2008),113501-113506.

[18] A.Mars , H.Essaidi, J.Ouerfelli (2015) Mater. Sci. Semicon. Proc. 40 319–324.

[19] H M Pathan and C D Lokhande, Bulletin of Material Science, Vol. 27(2), 2004, 85-111.